SACLANT ASW
RESEARCH CENTRE
REPORT

AN AMBIENT-NOISE MODEL
THAT INCLUDES COHERENT HYDROPHONE SUMMATION
FOR SONAR SYSTEM PERFORMANCE IN SHALLOW WATER

by

Rachel M. HAMSON and Ronald A. WAGSTAFF

15 JUNE 1983

NOV 8 1983

A

NORTH
ATLANTIC
TREATY
ORGANIZATION

LA SPEZIA, ITALY

83 11 08 011

AN AMBIENT-NOISE MODEL THAT INCLUDES COHERENT HYDROPHONE SUMMATION
FOR SONAR SYSTEM PERFORMANCE IN SHALLOW WATER

by

Rachel M. Hamson and Ronald A. Wagstaff

15 June 1983

This report has been prepared as part of Project 21.

APPROVED FOR DISTRIBUTION

RALPH R. GOODMAN
Director

TABLE OF CONTENTS

List of Figures

AN AMBIENT-NOISE MODEL THAT INCLUDES COHERENT HYDROPHONE SUMMATION
FOR SONAR SYSTEM PERFORMANCE IN SHALLOW WATER

by

Rachel M. Hamson and Ronald A. Wagstaff

ABSTRACT

A model (RANDI II) is described that predict noise levels and
directionalities in specified environmental/shipping conditions and
calculates the response of any arbitrary array of hydrophones to the noise
field. The model includes a shallow-water option based on normal-mode
propagation. The array response per ship is calculated by the addition of
the complex pressure of individual modes at each hydrophone, followed by
either coherent or incoherent summation of modes. Shallow-water wind noise
is provided by a wave-theory model for the correlation matrix between all
hydrophones of the array. Modelled results are compared with measured data
at three different sites, one in shallow water.

INTRODUCTION

A review of the underwater acoustic literature reveals the existence of a large number of ambient-noise models. Thirteen different models are listed in <1>. Some have general applications, others are intended specifically for the calculation of omnidirectional levels, horizontal or vertical directionalities, or the beam noise of an array. Some "models" are as simple as curves on a graph, while others are elaborate computer codes. However, to the knowledge of the authors, they all have one thing in common — they were developed with plane-wave propagation in mind.

This paper discusses the Research Ambient Noise Directionality II model (RANDI II) developed at SACLANTCEN. This was constructed with emphasis on the special problems caused by the shallow-water environment. The aim was to model both the ambient-noise field in such conditions and the performance of a general passive-sonar system operating in that field. The main feature of the model is its capability to calculate the response of any arbitrary array of hydrophones to an inhomogeneous incident field, such as that arising from the shallow-water propagation of shipping noise. At present several other noise models can do this for a single sensor by using data of amplitude (or propagation loss) versus range obtained from measurements or from a shallow-water propagation model. However, this cannot be done for an array unless the amplitude and phase information at each sensor are combined coherently in the array processing, which is what the RANDI II model does. The model can also handle simpler situations of deep-water ambient noise, where the plane-wave assumption is reasonable.

The RANDI II model contains two sources of noise — shipping and wind — that are dominant over a wide frequency range from a few hertz to several kilohertz. The environment around the array (or measurement site) can be divided into horizontal sectors of different propagation conditions (e.g. different bottom types or water depths in various directions from the array). Ships are entered at specific positions and moved by dead-reckoning for several time steps. The noise field and array response are calculated at each step. The array responses can be further processed, if desired, in the same way as an array output might be processed during measurements at sea. An estimate of the ambient-noise field thus obtained from array data, rather than the ambient-noise field created by the model itself, can be directly compared with estimates obtained at sea.

Chapter 1 gives a more detailed description of the model, particularly of the array-response calculation for the shallow-water option. Chapter 2 presents some typical output products of the model: horizontal directionality plots, line array responses, and spatial statistics. In Ch. 3 the modelled results for two specific areas are compared with experimental results from towed-array data. One area consists of a shallow-water/heavy-shipping region near the edge of the continental shelf, and the other is in a deeper basin containing one distinct shipping lane. Two different sites in this latter area have been modelled. As well as creating the appropriate noise fields for these environments, the model was used to simulate the towed-array measurements exactly as they were conducted at sea. The noise fields estimated from the simulated data are comparable with the measured estimates.
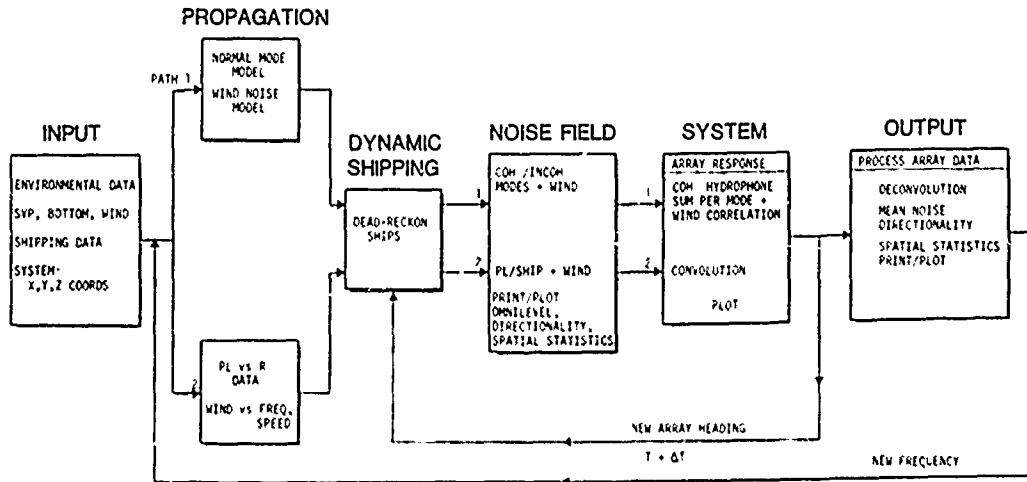
3

FIG. 1   SIMPLIFIED BLOCK DIAGRAM OF RANDI-II MODEL

1   MODEL DESCRIPTION

A block diagram of RANDI II is shown in Fig. 1. There are two paths through the model, corresponding to different methods of modelling propagation. The environmental data required depend on which path is selected and may consist of range-dependent sound-speed profiles and bottom conditions for each azimuthal sector, or just simple parameters for propagation-loss calculation. Shipping data are entered as latitude, longitude, speed, course, and length of each ship. An arbitrary array can be specified by its hydrophone coordinates, or an equally spaced line array can be specified by its hydrophone spacing and tilt angle.

Path 1 through the model is most suited to shallow water and uses SACLANTCEN's normal-mode propagation model, SNAP <2>, to calculate the acoustic field due to each ship at each hydrophone position in terms of the complex pressures of individual propagation modes. SACLANTCEN's surface-noise model (based on the theory of Kuperman and Ingenito <3>) has been implemented to calculate the contribution of wind noise. It models the generation of wind noise by an infinite layer of surface (point) sources and represents wind noise propagation to the array by the use of the full solution of the wave equation (i.e. discrete normal-modes plus the continuous spectrum or "near-field" of the sources). This model contains a combination of SNAP and a fast field program <4>, the latter providing the continuous-mode contribution. The output of the wind model is a matrix of complex correlation coefficients between all hydrophones of the array.

Source levels of both shipping and wind are required in order to obtain the combined noise field from the data produced by these "unit source" models. An "average" ship has been defined as one with a speed of 12 kn and a length of 300 ft (91 m); to this ship is assigned a source level of X dB as a function of frequency, f. The noise source levels of the actual ships in the model are then calculated, on the basis of their individual speeds and lengths, by the equation

$$L = X(f) + 60 \log_{10} \left(\frac{V}{12}\right) + 20 \log_{10} \left(\frac{L}{300}\right) \text{ dB} ,$$

where   V = speed in knots,

L = length in feet.

This is an empirical expression for the dependence of noise on speed and length that is similar to expressions given on p. 277 of <5>, (where the ship's displacement tonnage is used instead of its length). A set of values of X(f) was initially obtained by comparing the modelled omnidirectional noise levels with measurements for a particular site. That same set has since been used at several sites in very different propagation conditions and resulted in good agreement (within 3 dB) between modelled and measured levels.

For the source level of wind noise, which is a function of wind speed and frequency, recent results obtained by Wilson <6> for a frequency range of 50 Hz to 1000 Hz have been directly implemented in the model.

At this point the noise field due to a particular azimuthal distribution of ships and a specified wind speed is available, and one point (one hydrophone position) can be selected at which to make a horizontal directionality plot of the field. The normal-modes per ship can be combined either coherently (vectorially) or incoherently. The field, F, at a selected point (r_s, Z) due to ship s at range r_s and bearing B_s is given, by coherent or incoherent mode summation respectively, by:

$$F(B_s) = L_s \left| \sum_m P_m(r_s, Z) \right|^2$$

or

$$= L_s \sum_m \left| P_m(r_s, Z) \right|^2 ,$$

where

Z = depth of observation point,

P_m = complex pressure of the mth propagation mode,

L_s = source level (in power) of ship, s.

(The array response calculation of the next block, however, will still require the separate modal pressures.)

Path 2 through the model (Fig. 1) is more suitable for deep water or higher frequencies, since plane-wave propagation for shipping noise is assumed. Propagation-loss data from measurements or from other propagation models can be read, or equations for loss versus range can be used. Source levels for shipping are calculated as for path 1. Omnidirectional wind noise is calculated from empirical equations as a function of frequency and wind speed. These were obtained by fitting to the curves drawn from modern measurements of deep-water wind-generated noise (p. 71 of <5>), although wind speed is used as a parameter rather than the wind force given in the reference.

The output at this stage is a plot of the horizontal noise field, with the ships in their initial positions. This has the form of wind background noise with noise spikes in the direction of the ships (see the first plot of Fig. 2, for example).

The array-response calculation then follows its complexity depends on the selected path. For path 1, the complex pressure of each normal mode is summed over all hydrophones. Each hydrophone may have its own complex weighting, $W_n e^{i\phi_n}$. The W_n's provide the amplitude weighting of the array and can be chosen, for example, for Hann shading or set equal to unity for a uniform array. The ϕ_n's can be calculated, if desired, for conventional beam steering. For a general arbitrary array with hydrophone positions in spherical polar coordinates (r_n, θ_n, ψ_n) steered in a general direction (θ_s, ψ_s), these phase weightings would be given by

$$\phi_n = \frac{2\pi}{\lambda} r_n (\sin\theta_s \sin\theta_n \cos(\psi_s - \psi_n) + \cos\theta_s \cos\theta_n),$$

for wavelength, λ.

6

For the particular case of an equally spaced horizontal line array with spacing d, steered in the horizontal plane to direction ψ_s, this reduces to

$$\phi_n = \frac{2\pi}{\lambda} \, nd \, \cos(\psi_s - h),$$

where h is the array orientation (heading).

However, any specified array processing can be incorporated via the weightings W_n and ϕ_n. For example, the output of signal-processing algorithms that calculate optimum weightings could be entered.

The power response of the array to one ship, s, is given, by coherent or incoherent combination of modes respectively, by:

$$L_s \left| \sum_{m=1}^{M} \sum_{n=1}^{N} W_n \, e^{i\phi_n} \, P_m(r_n, Z_n) \right|^2$$

or

$$L_s \sum_{m=1}^{M} \left| \sum_{n=1}^{N} W_n \, e^{i\phi_n} \, P_m(r_n, Z_n) \right|^2 ,$$

where

N	=	number of hydrophones,
M	=	number of modes,
$P_m(r_n, Z_n)$	=	complex pressure of the mth mode at ,ydrophone n due to this ship,
r_n	=	range from ship to hydrophone,
Z_n	=	depth of hydrophone.

This calculation is carried out for each ship (and for each steering direction if beamforming is being simulated) and the array's power responses are summed over all ships.

The array's response to wind noise for this path l is calculated from the complex correlation matrix $[C_{lj}]$ produced by the shallow-water surface-noise model, by the double summation

$$\sum_{l=1}^{N} \sum_{j=1}^{N} W_l \, W_j \, e^{i(\phi_l - \phi_j)} \, C_{lj}.$$

This contribution, after multiplication by the appropriate wind source level from ‹6›, is added to the array's response to shipping noise.

This type of array-response calculation takes full account of the inhomogeneous acoustic field arising from the shallow-water propagation of both shipping and wind noise, and is applicable to a completely arbitrary array of hydrophones.

For path 2, the array-response calculation is much simpler (and faster): the directional noise field due to all ships and wind is convolved with either the two-dimensional or three-dimensional beam pattern of the array.

At this point in the model, time is incremented, the new ship positions are calculated by dead reckoning, and a new directional noise field and array response calculated. The model has been used at SACLANTCEN for the particular case of a horizontal array to simulate experiments at sea in which an array is towed on a polygonal series of headings and noise is measured during each separate orientation of the array. This procedure is easily simulated in the model by changing the array heading for each new set of ship positions.

The last block of Fig. 1 (marked 'output') represents a processing method for the deconvolution of line-array data <7>. This is used at sea to estimate the horizontal directionality of ambient noise and obtain statistics from towed-array ambiguous data. It can be applied to line-array response data from the model, as will be described in Ch. 2.

2   OUTPUT PRODUCTS OF THE MODEL

Some examples of the outputs from the model for the shallow-water path 1 are given in Fig. 2. This shows array responses to the 150 Hz ambient noise field in 140 m of water due to 13 ships at ranges of 40 to 100 n.mi and 10 kn of wind. The plot in Fig. 2a is the directional field in the horizontal plane, showing shipping noise spikes against the omnidirectional wind background. The plot in Fig. 2b is the response of a horizontal Hann-shaded array of 40 elements, oriented in the direction of the arrow and scanned around 180°. The two curves on the plot correspond to incoherent summing (solid curve) and coherent summing (dotted curve) of the normal modes per ship. Note the maximum response to the dominant ship spike to the northeast, which is of course ambiguous to the southwest.

The plots in Figs. 2c and d are the responses of a vertical array of 15 hydrophones at the same position, to shipping noise only (on the left) and to both shipping and wind (on the right). These are plotted in the vertical plane, as the array is steered from the surface direction to the bottom direction. Again, two curves are shown: for incoherent and coherent mode summations. The main response of the vertical array to shipping alone occurs at about $\pm 10°$ from the horizontal. Addition of wind via the shallow-water surface-noise model increases the vertical arrivals from both surface and bottom to an extent dependent on the particular sound-speed profile and bottom type modelled.

Figure 3 shows more clearly the differences that can occur between incoherent and coherent additions of the normal modes per ship. A directional noise field due to 280 ships at a particular shallow-water site is shown in the Fig. 3a. The plots in Figs. 3b and c show the responses of a horizontal array to this noise field when the array is placed at two positions 1 km apart. Note that with incoherent summing (solid curves) this small change in the range of each ship causes a negligible difference in the response. Coherent summing (dotted curves), however, changes it significantly, by up to 15 dB, and in the second position this method fails to "detect" the noise from the ship that is dominant to the southwest. Similar fluctuations in the coherent result would occur with small changes in other parameters, such as frequency, source depths, and array depth. All of these cause the relative phases of the modes to change. Coherent (or vectorial) addition of modes represents the real situation at an instant; incoherent addition gives an average result that is more suitable for simulating array measurements over a period (during which the ships are moving) and for a finite bandwidth.

Other outputs of the model are illustrated in Fig. 4. The horizontal noise field at any instant is plotted as a distribution of noise spikes, as in Fig. 4a. This particular example is for the noise due to 70 ships to the north of the measurement site. The field can be smoothed with an unambiguous "beam" of specified width (5° in this example) and sidelobe level to give the curve shown. This result corresponds closely to the output of an array with a 5° unambiguous beam operating in this noise field. Such results are available at every time step of the model.

Over the total period modelled, typically 10 hours, the spatially smoothed fields at each step are averaged to produce the mean noise field. An

example is plotted in Fig. 4b, which was obtained by averaging nine instantaneous smoothed fields, that given by the curve in Fig. 4a being one of them. The mean field is an important product of the model and gives more information on the noise at a given site than does the average omnidirectional level so common in the literature. It gives an average level measured by a sonar system having a 5° wide unambiguous beam, and it gives it for every degree of the 360° azimuth. The omnidirectional level is obtained by summing over all azimuths.

Another product of the model involves the spatial statistics of the noise in the form of azimuthal anisotropy cumulative distribution function (AACDF) plots. An example is given in Fig. 4c. This is a plot of beamwidth against the percentage of azimuth and is generated in the following manner. The "spiked" fields at each time step are sampled with beams of varying widths. The beam outputs are accumulated according to level and width during the total period. The resulting distribution functions are plotted as curves of equal level. This sort of plot has a direct application in sonar performance prediction. For example, we see that a 3° beam would measure a noise level of less than 53 dB for 50% of the azimuth at this site, or that a 7° beam would measure less than 63 dB for 80% of the azimuth. These plots can be made for the whole 360° azimuth or for selected sectors. The example in Fig. 4c is for the quadrant from north to east.

AACDF plots are also useful for verifying noise models. They are measures of the noise anisotropy and can be used to determine whether the ships are correctly distributed in the model. For example, a shipping lane at a given range on one side of the measurement site could have 10 ships within a sector, each with a source level of X dB, or there could be 100 ships each with a source level of X-10 dB. The omnidirectional levels and average horizontal directionalities would be the same, but the AACDF plots would differ considerably. With the 100 ships the curves would be fairly flat, showing little variation in noise level within the sector. With the 10 ships the curves would be steeper, giving high variation in level where beams can "fit between" the ships. AACDF's can also be generated from line-array data after deconvolution. This is carried out by the final block in the flow diagram (Fig. 1) and can be applied both to array data from the model and from measurements at sea, providing a good basis for comparing modelled results with experimental results.

THEORETICAL ARRAY RESPONSES
TO SHALLOW WATER AMBIENT NOISE

a) NOISE FIELD (SHIPPING+WIND) HORIZONTAL DIRECTIONALITY

b) HORIZONTAL ARRAY RESPONSE

c) VERTICAL ARRAY RESPONSE (TO SHIPPING ONLY)

d) VERTICAL ARRAY RESPONSE

FREQUENCY 150Hz
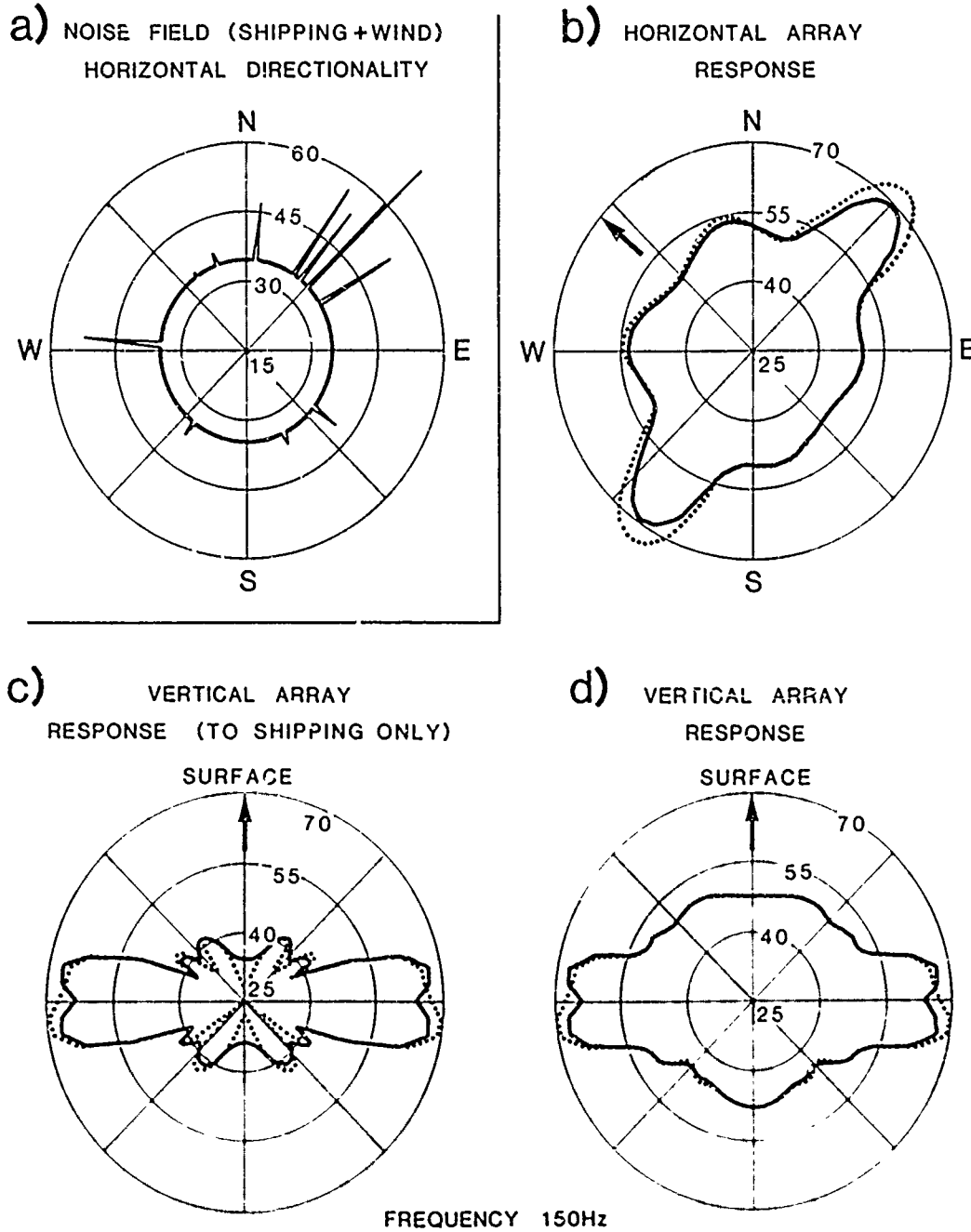
FIG. 2 ARRAY RESPONSES TO SHALLOW-WATER AMBIENT NOISE FIELD

11

HORIZONTAL ARRAY RESPONSES AT A SHALLOW WATER SITE

a) NOISE FIELD HORIZONTAL DIRECTIONALITY

FREQ 150Hz

b) ARRAY RESPONSE

c) ARRAY RESPONSE

INCOHERENT MODE SUM

COHERENT MODE SUM

1km DIFFERENCE IN ARRAY POSITIONS
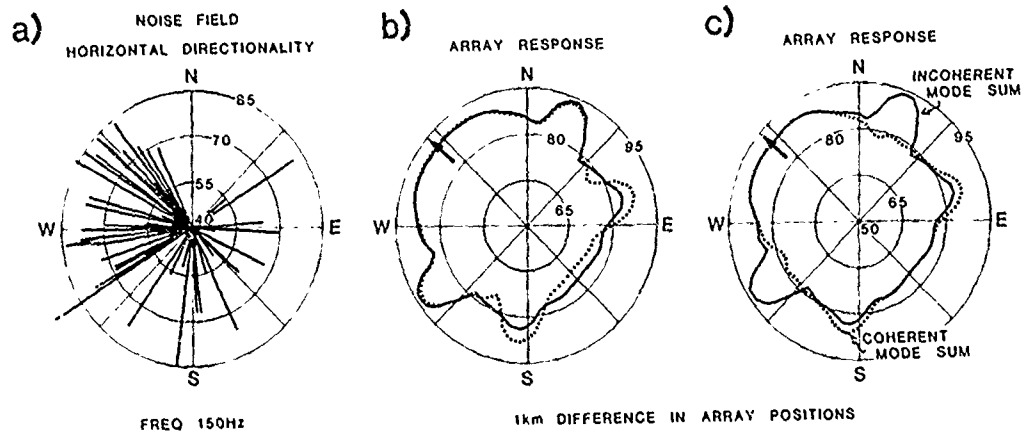
FIG. 3   HORIZONTAL LINE-ARRAY RESPONSES, SHOWING RESULTS FOR COHERENT
AND INCOHERENT MODE SUMMATION

a) HORIZONTAL DIRECTIONALITY

b) HORIZONTAL DIRECTIONALITY

c)
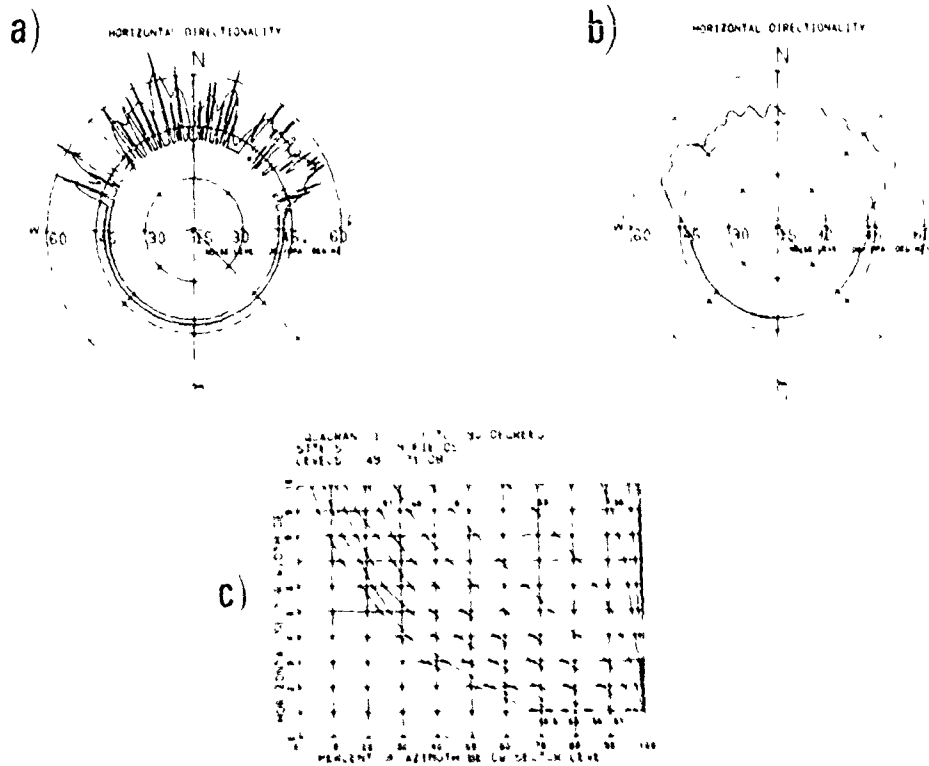
FIG. 4   EXAMPLES OF (a) PLOT OF THE INSTANTANEOUS NOISE FIELD, (b) PLOT OF
THE TEMPORALLY AND SPATIALLY AVERAGED HORIZONTAL DIRECTIONALITY,
AND (c) AACDF PLOT FOR THE QUADRANT FROM 0° TO 90°

3   COMPARISON WITH MEASUREMENTS

In this chapter the modelled results for specified sites in two areas are compared with ambient-noise estimates obtained from recent towed-array experiments. In the first area (area A), which consists of a small basin of approximately 1400 m water depth, the ambient noise at two sites was modelled using the simple path 2 of the model, with empirical propagation-loss equations. The second area (area B) is in shallow water (130 m depth), where the noise at a single site was modelled using path 1 with appropriate environmental conditions for the normal-mode model, SNAP, and the shallow-water wind-noise model. The array used in all measurements and in the model contained 40 elements spaced at 1.5 m.

3.1   Area A

Figure 5 shows the locations and courses of 70 ships in the first area and the two measurement sites. The shipping data were obtained by aerial surveillance at the time of the measurements. Topographic shielding blocked off all noise from ships beyond those plotted. This close-range, fairly deep water situation is ideally suited to the second option of the model with its simple propagation-loss equations of the form $A \log R + \alpha R$, where R is range in metres, α is a frequency-dependent absorption coefficient, and A is a constant.

For site 1, which is south of the shipping lane, the azimuth was divided into two sectors, one from northwest to northeast looking across the deep water of the basin and using A=20 (i.e. spherical spreading), and the other looking in all other directions across shallower water (about 900 m) using A=15. A wind speed of 3 kn was used in the model (corresponding to that prevailing during the measurements) and nine different array headings over a period of nine hours simulated the polygon executed at sea. The model was run for several frequencies.

Figure 6 illustrates some of the modelled and measured results for the 500 Hz ambient noise at site 1. The lefthand column of Fig. 6a shows three examples of the instantaneous noise field generated by the model at one hour intervals, with spikes to the north in the direction of the shipping lane. The second column shows the simulated response of the array to these fields for three array headings. The third column gives examples of measured beam responses obtained at sea. Since the ship movements in the model are estimated by dead-reckoning, the modelled and measured beam responses cannot be compared on a beam-to-beam basis. However, there are general similarities of pattern and level.

Figure 6b shows the plots of horizontal noise directionality obtained from modelled and measured data of the type illustrated in the corresponding columns of Fig 6a. The first plot is the mean modelled field over nine hours, obtained by spatially smoothing each instantaneous spiked field over 5° and averaging the results. The second is the estimate of the horizontal field obtained by deconvolution and ambiguity resolution of the nine sets of array response data. The third plot is the estimate obtained at sea from towed-array data. The omnidirectional levels are written below each plot.

SHIPPING : RELATIVE POSITIONS and COURSES
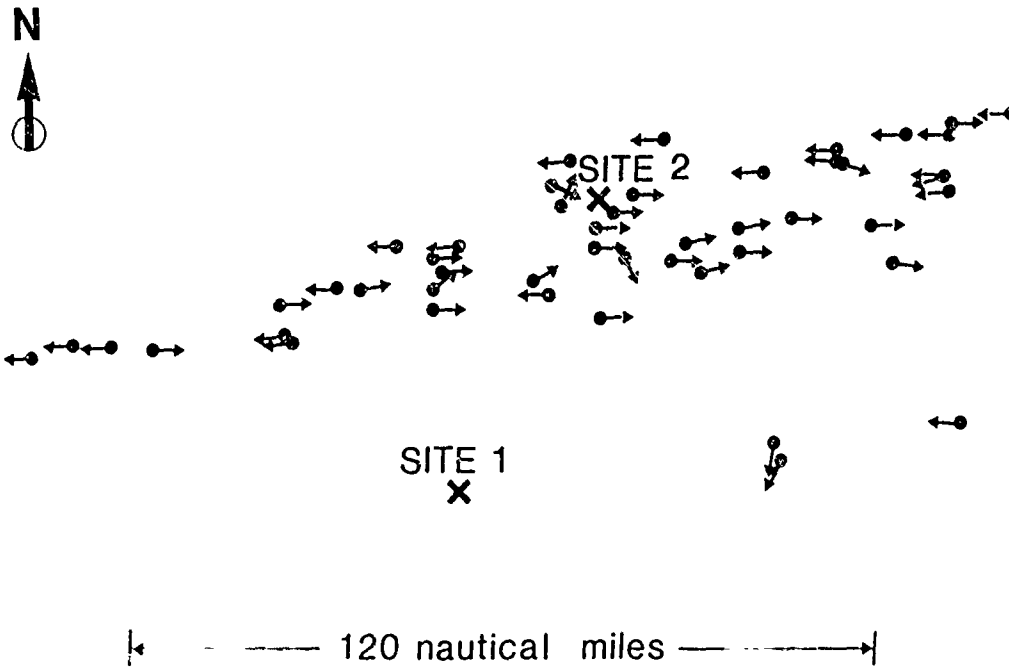
FIG. 5 AREA A: MEASUREMENT SITES AND NEARBY SHIPPING DISTRIBUTION
DURING AMBIENT NOISE MEASUREMENTS

a)

MODELLED

FIELD   BEAM RESPONSE   MEASURED BEAM RESPONSE
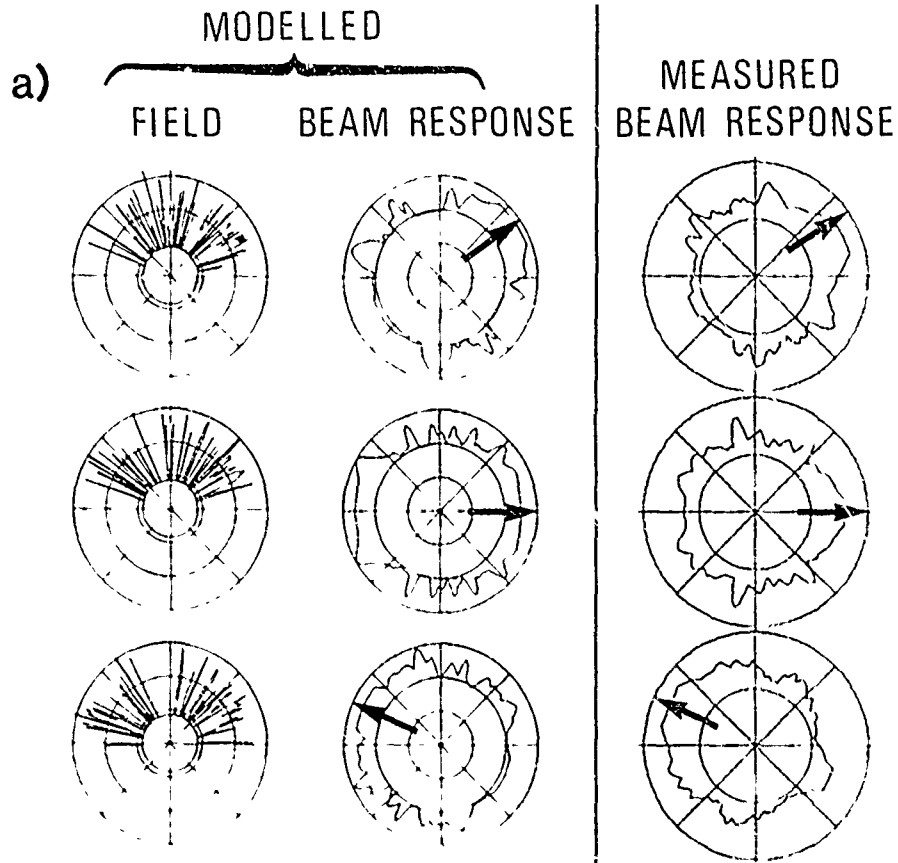
FIG. 6a   *EXAMPLES OF SIMULATED AND MEASURED RESULTS FOR AMBIENT-NOISE MEASUREMENTS BY A TOWED ARRAY AT SITE 1. Noise field and beam response data at 500 Hz for three of the nine measurement periods are given.*

b)   HORIZONTAL DIRECTIONALITY
AREA A, SITE1

500 Hz 70 5 dB	500 Hz 70 6 dB	500 Hz 69 8 dB
MODELLED FIELD	SIMULATED	MEASURED SEPT 80

NOISE LEVEL (dB µPa² DEG Hz)

FIG. 6b   *AMBIENT-NOISE HORIZONTAL DIRECTIONALITY PATTERNS FOR 500 Hz OBTAINED FROM THE NOISE MODEL (left hand plot), FROM THE SIMULATED MEASUREMENTS (centre plot), AND FROM THE ACTUAL MEASUREMENTS (right hand plot) BY A TOWED ARRAY AT SITE 1.*

The last two noise-field estimates in Fig. 6b are based on the simulation of the array measurements and on the actual array measurements; both had ambiguities in the input data that needed to be resolved to produce these noise-field estimates. They are therefore directly comparable. It is seen that there is good agreement between them, both in the estimate of the horizontal pattern and in the omnidirectional level. If the simulated estimate of the centre plot is now compared with the 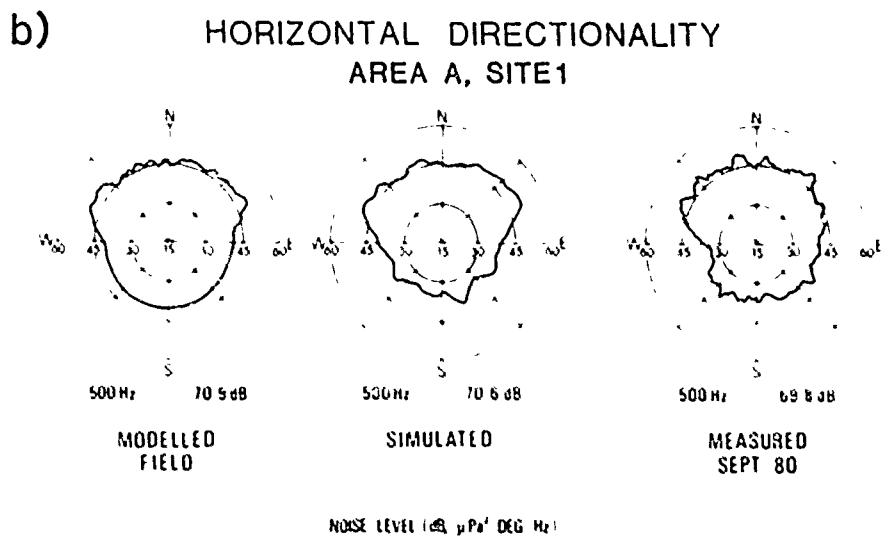mean modelled field in the left-hand plot there is also a reasonable degree of similarity. This suggests that both the array and the processing method have done a reasonable job of estimation.

A further comparison between model and measurement can be made with the AACDF plots. Figure 7 compares the 500 Hz plot from the measurement (solid curves) with the 500 Hz plot from the model (dashed curves). There is good agreement in gradients and spacings of the curves, the maximum discrepancy for a given beamwidth and level being about 10%. These plots were obtained from the measured and simulated array outputs by deconvolution followed by reconvolution with arrays of different beamwidths. The line-array ambiguity however was not resolved; hence this AACDF plot can be directly used to give the performance of other horizontal arrays (of beamwidths up to 10°) operating in the same area.

For site 2, which is situated in the shipping lane (see Fig. 5), one propagation-loss equation (with A=20, for spherical spreading) was used for all directions. The ship source levels were the same as those used at site 1. Figure 8, which is of the same form as Fig. 6b, gives the horizontal noise directionality at 480 Hz according to the modelled field (averaged over nine hours), the simulated estimate, and the measured estimate. The omnidirectional levels are given under each plot. The three noise patterns are in agreement, all showing the highest noise levels in the east-west directions along the shipping lane. There is good agreement in omnidirectional noise level between simulation and experiment at site 2.

3.2 Area B (shallow water)

Now we consider the more complicated case of a shallow-water site near the edge of the continental shelf, with opportunities for long-range propagation from both shallow and deeper water. Figure 9 shows the location of this site in 130 m water depth. It also shows the distribution of 280 ships, as obtained by aerial surveillance during a previous trial in the same area and not on the actual day of measurements. In the shallow-water region, to about 200 m depth, the bottom is composed of sand and rock. Core samples in this part of the area indicate a hard bottom, with a sound speed of the order of 1800 m/s. Previous propagation-model studies <8> have resulted in a set of average bottom parameters (for density, compressional speed and attenuation) and have found it necessary to include shear loss to obtain agreement with measured propagation loss. Away from the shelf the bottom is composed of mud and, as water depth increases, has a lesser effect on propagation.

For ambient-noise modelling using path 1 the environment around this site was divided into two azimuthal sectors of different propagation conditions (see dashed line on Fig. 9), one between 210° through 360° to 060° having a
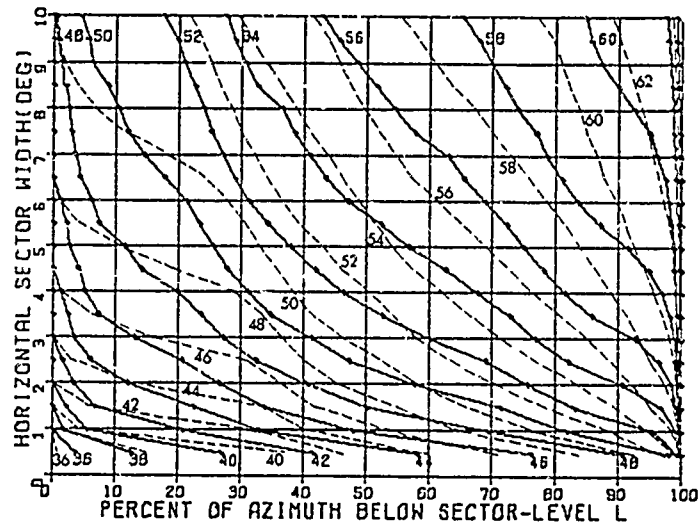
FIG. 7   AZIMUTHAL ANISOTROPY CUMULATIVE DISTRIBUTION FUNCTION PLOTS FOR
        THE 500 Hz NOISE AT SITE 1 FROM THE MEASUREMENTS (————) AND
        FROM THE MODEL (-----).

HORIZONTAL DIRECTIONALITY
AREA A, SITE 2

MODELLED   SIMULATED   MEASURED
FIELD

480 Hz   75 0 dB   480 Hz   74 9 dB   480 Hz   76 2 dB

NOISE LEVEL (dB μPa² OEG Hz)

FIG. 8   AMBIENT-NOISE HORIZONTAL DIRECTIONALITY PATTERNS FOR 500 Hz
        OBTAINED FROM THE NOISE MODEL (left hand plot), FROM THE
        SIMULATED MEASUREMENTS (centre plot), AND FROM THE ACTUAL
        MEASUREMENTS (right hand plot) BY A TOWED ARRAY AT SITE 2.

17

FIG. 9 AREA B: MEASUREMENT SITE, BATHYMETRY AND SHIPPING DISTRIBUTION.

constant water depth, and the other, looking southeast, having an increasing water depth away from the site. The normal-mode model (SNAP) 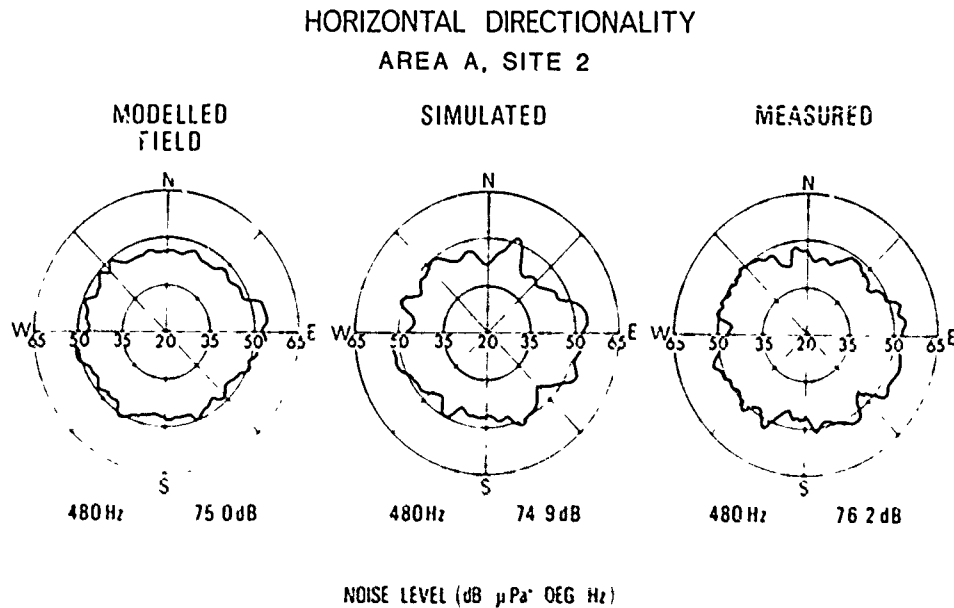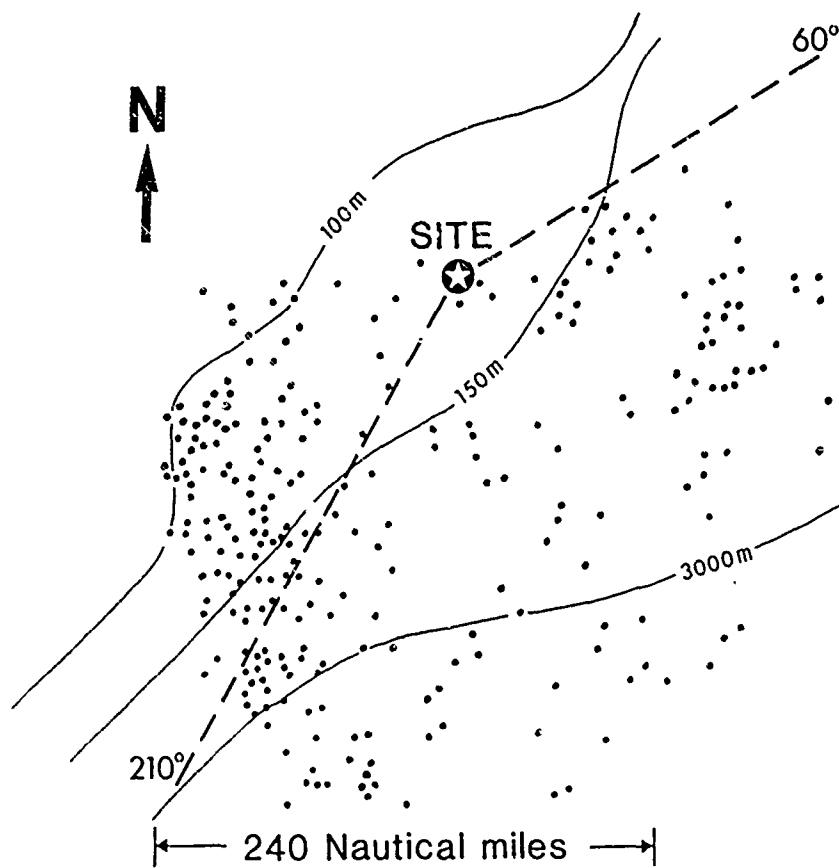was run separately for the two sectors, its range-dependent version being used for the second sector to take account of changing water depth and bottom type. A single sound-speed profile taken at the site during the measurements was used for both runs. This showed a thermocline down to 50 m depth. The mode pressure data generated by SNAP was stored for use by the ambient-noise model. The shallow-water wind-noise model was run with the same environmental data to produce the wind-noise correlation matrix. Wind speeds during the nine-hour measurement period varied from 12 to 25 kn. The array was towed at 50 m depth on nine different headings to form a polygon.

Path 1 of RANDI II was run to create the noise field at the site and to simulate the experiment. The ship source levels used were the same as in area A. The resulting horizontal directionalities for a freqency of 150 Hz are shown in Fig. 10, which is of the same form as Fig. 6b. Incoherent mode summation was used for both the field and array response calculations in the model. The agreement between the simulated and measured directionalities is good: both plots show high noise levels to the east and south in the directions of deep water and towards the high density of ships closeby to the east; low levels are seen to the northeast. The very high concentration of ships to the southwest is not especially dominant in either the modelled or measured results, probably due to the poorer propagation in shallow water. The model was also run using coherent combination of the modes per ship. This gave very similar results to those of Fig. 10, indicating that the effect of phase differences between modes had been averaged out over the period modelled.

Figure 11 gives the 150 Hz AACDF plots from the simulated (solid curves) and measured (dashed c..ves) data at the site. These show very good agreement in the spacings and gradients of the curves and in the actual noise levels. For a given beamwidth and level, the discrepancy is generally less than 8%. Thus the shipping distribution and the relative contributions of shipping and wind noise in the model seem to be reasonable.

Agreement between the simulated and measured estimates of the noise field indicate that the modelled field itself is close to the real ambient noise field (or that existing at the time of the measurement). The noise response of other sonar systems operating at this site could therefore be predicted with some confidence.

19

HORIZONTAL DIRECTIONALITY

AREA B

MODELLED FIELD   SIMULATED   MEASURED

150Hz   80.3dB   150Hz   81.2dB   150Hz   77.9dB

NOISE LEVEL (dB//μPa²/deg Hz)

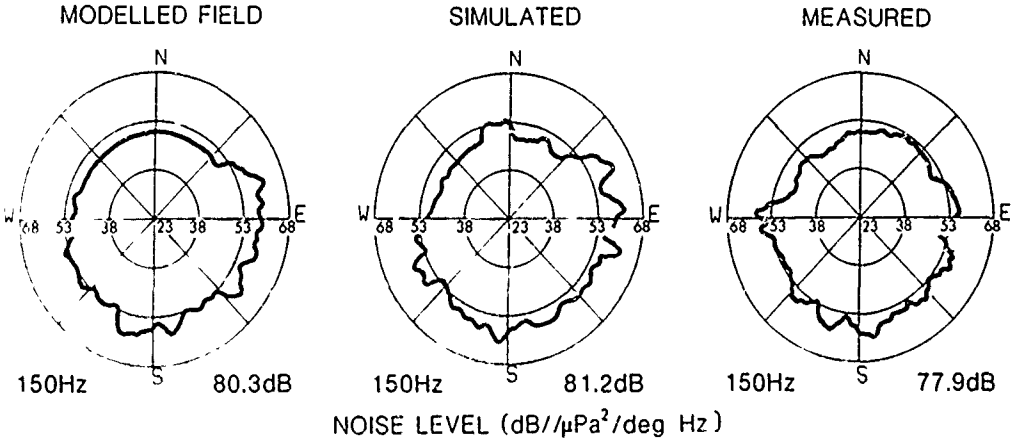FIG. 10 AMBIENT-NOISE HORIZONTAL DIRECTIONALITY PATTERNS FOR 150 Hz
OBTAINED FROM THE NOISE MODEL (left hand plot), FROM THE
SIMULATED MEASUREMENTS (centre plot), AND FROM THE ACTUAL
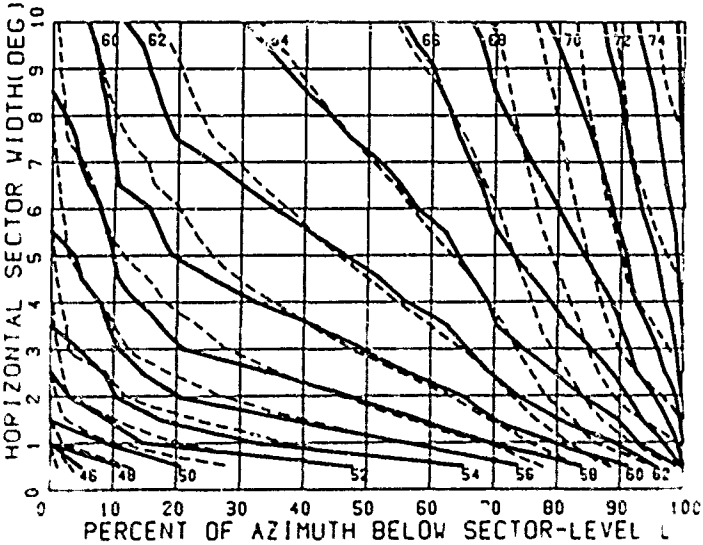MEASUREMENTS (right hand plot) BY A TOWED ARRAY AT A SITE
IN AREA B.

FIG. 11 AZIMUTHAL ANISOTROPY CUMULATIVE DISTRIBUTION FUNCTION PLOTS
FOR THE 150 Hz NOISE AT A SITE IN AREA B FROM THE MODEL
(———) AND FROM THE MEASUREMENTS (-----).

<u>CONCLUSIONS</u>

The RANDI II ambient-noise model has been described and used to model
ambient noise and array responses in two areas. Its special feature is the
capability to carry out coherent hydrophone summations of the complex
pressures of individual propagation modes, and to combine these in the
processing of an arbitrary array. This is important in shallow-water
situations.

The modelled results for two areas, one in shallow water, have been
compared with estimates of ambient noise made from recent measurements with
a towed array. Comparisons made on the basis of omnidirectional noise
level, horizontal directionality, and the spatial statistics of the noise,
show good agreement.

The model could be further evaluated by carrying out simultaneous vertical
and horizontal array measurements in shallow water of known bottom type in
order to check its three-dimensional capability. Another aspect that needs
to be investigated separately is the modelling of shallow-water wind noise
and its source levels. This would require a set of measurements of
wind-only noise in shallow water and various sea-states.

REFERENCES

1. ETTER, P.C. and FLUM, R.S., Sr. A survey of underwater acoustic
    models and environmental-acoustic data banks, ASWR-80-115.
    Washington, D.C., Anti-submarine Warfare Systems Project Office, 1980.
    [AD B 053 767]

2. JENSEN, F. and FERLA, M.C. SNAP: the SACLANTCEN normal-mode acoustic
    propagation model, SACLANTCEN SM-121. La Spezia, Italy, SACLANT ASW
    Research Centre, 1979. [AD A 067 256]

3. KUPERMAN, W. and INGENITO, F. Spatial correlation of surface
    generated noise in a stratified ocean. Journal of the Acoustical
    Society of America, 67, 1980: 1988-1996.

4. KUTSCHALE, H.W. Rapid computation by wave theory of propagation loss
    in the Arctic Ocean, CU-8-73. Palisades, N.Y., Columbia University,
    1973.

5. ROSS, D. Mechanics of Underwater Noise. Oxford, U.K., Pergamon
    Press, 1976.

6. WILSON, J.H. Low-frequency wind-generated noise produced by the
    impact of spray with the ocean's surface. Journal of the Acoustical
    Society of America, 68, 1980: 952-956.

7. WAGSTAFF, R.A. Iterative technique for ambient noise horizontal
    directionality estimation from towed line array data. Journal of the
    Acoustical Society of America, 63, 1978: 1287-1294.

8. JENSEN, F.B. and KUPERMAN, W.A. Environmental acoustic modelling at
    SACLANTCEN, SACLANTCEN SR-34. La Spezia, Italy, SACLANT ASW Research
    Centre, 1979. [AD A 081 853]

INITIAL DISTRIBUTION

	Copies		Copies
MINISTRIES OF DEFENCE		**SCNR FOR SACLANTCEN**	
MOD Belgium	2	SCNR Belgium	1
DND Canada	10	SCNR Canada	1
CHOD Denmark	8	SCNR Denmark	1
MOD France	8	SCNR Germany	1
MOD Germany	15	SCNR Greece	1
MOD Greece	11	SCNR Italy	1
MOD Italy	10	SCNR Netherlands	1
MOD Netherlands	12	SCNR Norway	1
CHOD Norway	10	SCNR Portugal	1
MOD Portugal	2	SCNR Turkey	1
MOD Turkey	5	SCNR U.K.	1
MOD U.K.	16	SCNR U.S.	2
SECDEF U.S.	65	SECGEN Rep. SCNR	1
		NAMILCOM Rep. SCNR	1
NATO AUTHORITIES			
		NATIONAL LIAISON OFFICERS	
Defence Planning Committee	3	NLO Canada	1
NAMILCOM	2	NLO Denmark	1
SACLANT	10	NLO Germany	1
SACLANTREPEUR	1	NLO Italy	1
CINCWESTLANT/COMOCEANLANT	1	NLO U.K.	1
COMSTRIKFLTANT	1	NLO U.S.	1
COMIBERLANT	1		
CINCEASTLANT	1		
COMSUBACLANT	1	**NLR TO SACLANT**	
COMMAIREASTLANT	1	NLR Belgium	1
SACEUR	2	NLR Canada	1
CINCNORTH	1	NLR Denmark	1
CINCSOUTH	1	NLR Germany	1
COMNAVSOUTH	1	NLR Greece	1
COMSTRIKFORSOUTH	1	NLR Italy	1
COMEDCENT	1	NLR Netherlands	1
COMMARAIRMED	1	NLR Norway	1
CINCHAN	1	NLR Portugal	1
		NLR Turkey	1
		NLR UK	1
		NLR US	1
		Total initial distribution	238
		SACLANTCEN Library	10
		Stock	32
		Total number of copies	280